International Journal of Fluid Mechanics Research, Vol. 32, No. 3, 2005

Transient Free Convection Flow of a Micropolar Fluid Over a Vertical Surface[†]

H. M. Duwairi
Mechanical Engineering Department, Faculty of Engineering and Technology
The University of Jordan, Amman – Jordan

A. J. Chamkha
Manufacturing Engineering Department
The Public Authority for Applied Education and Training
Shuweikh, 70654, Kuwait
email: achamkha@yahoo.com

In recent years, the dynamics of micropolar fluids, originated from the theory of Eringen, has been a popular area of research. As the fluids consist of randomly oriented molecules, and as each volume element of the fluid has translational as well as rotational motions, the analysis of physical problems in these fluids has revealed several interesting phenomena, which are not found in Newtonian fluids. The present study presents a numerical study for transient natural convection heat transfer of a micropolar boundary layer flow near a vertical isothermal surface. The governing equations are formulated and solved numerically using the MackCormak's technique. A comparison with previously published results on special cases of the problem shows excellent agreement. Representative results for the velocity, micro-rotation and temperature profiles are shown graphically for different values of material parameters. In general, it is found that the temperature increases inside the boundary layer for the micropolar flows as compared to the Newtonian flows.

* * *

Nomenclature

B	dimensionless material parameter;
C_f	local coefficient of friction;
C_p	specific heat of the fluid at constant pressure;
g	magnitude of acceleration due to gravity;
Gr	Grashof number, $\mathrm{g}\beta(T_w - T_\infty)L^3/\nu^2$;
h	heat transfer coefficient;

[†]Received 21.06.2005.

ISSN 1064-2277

j microinertia density;
k thermal conductivity;
L characteristic length of plate;
n micro-gyration constant;
N micro-rotation parameter;
Nu_x local Nusselt number;
Pr Prandtl number, ν/α;
R vortex viscosity parameter;
τ dimensionless time;
T temperature;
T_w wall temperature;
T_∞ ambient fluid temperature;
u, v dimensionless velocity components along x- and y-axes;
x, y dimensionless coordinates.

Greek Symbols

α thermal diffusivity;
β coefficient in the density;
γ spin gradient viscosity;
κ vortex viscosity;
λ dimensionless material parameter;
θ non-dimensional temperature;
μ dynamic viscosity;
ν kinematic viscosity;
ρ fluid density;
ω micro-rotation component.

Subscripts

w wall surface;
∞ free stream condition.

Superscripts

$^-$ dimensional variables.

Introduction

Recently, micropolar fluid flows and heat transfer have received much attention because the traditional Newtonian fluid theory cannot precisely describe the characteristics of a fluid with suspended particles. The theory of micropolar fluids and thermo-micropolar fluids developed by Eringn [1, 2] can be used to explain these characteristics in certain fluids such as exotic lubricants, colloidal suspensions, or polymeric fluids, liquid crystals and animal blood. Micropolar fluids exhibit certain microscopic effects arising from local structure and micro-rotation of fluid elements. An excellent review about micropolar fluid mechanics was provided by Ariman et al. [3, 4].

In the past decades, the researchers have focused mainly on the heat transfer of micropolar fluid flow over flat plates [5–7] or regular surfaces [8, 9]. Recently, Yao [10] studied natural convection

heat transfer from wavy surfaces. Cheng and Wang [11] studied the effect of wavy surfaces on forced convection heat transfer for micropolar fluids. They found that increasing the micropolar fluid parameter resulted in decreasing the heat transfer rates and increasing the local coefficient of friction and the hydrodynamic and thermal boundary layer thicknesses.

More recently, Bhargava and Takhar [12] studied micropolar boundary layer near a stagnation point on a moving wall. They concluded that the temperature inside boundary layer for a micropolar fluid increased compared to Newtonian flows. Mansour et al. [13] studied heat and mass transfer effects on magnetohydrodynamic flow of a micropolar fluid on a circular cylinder with uniform heat and mass flux. Their results indicated that micropolar fluids displayed a reduction in drag as well as heat transfer when compared with Newtonian fluids. Kelson and Desseaux [14] reported selfsimilar solutions for boundary layer flow of micropolar fluids driven by a stretching sheet with uniform suction or blowing through the surface. Ibrahim and Hassanien [15] obtaind local similarity solutions for mixed convection boundary layer flow of a micropolar fluid on horizontal flat plates with variable surface temperature. Kim and Lee [16] developed analytical studies on MHD oscillatory flow of a micropolar fluid over a vertical porous plate. The effects of non-zero values of micro-gyration vector on the velocity and temperature fields across the boundary layer were studied using the method of small perturbation approximation. Elbarbary and Elgazery [17] studied the effect of thermal radiation and variable viscosity and thermal conductivity on micropolar fluids using the Chebshev finite difference method. Their results showed that the variable viscosity and thermal conductivity in the presence of thermal radiation had significant influence on the velocity, angular velocity and the temperature profiles as well as the shear stress, couple shear stress and the Nusselt number.

The aim of the present work is to analyze transient and steady natural convection heat transfer problems adjacent to a vertical semi-infinite plate for an incompressible micropolar fluid. The governing equations for this investigation are written in dimensionless form using a set of dimensionless variables and solved numerically using the MackCormak's technique. Numerical results for the velocity, micro-rotation and temperature profiles as well as the local coefficient of friction and local Nusselt number under the effect of vortex viscosity parameter, spin gradient viscosity parameter, material parameter and the micro-gyration parameter are presented by means of graphs and tables.

1. Mathematical Formulation

Consider laminar free convection boundary layer flow of a micropolar fluid over an isothermal vertical flat plate which is heated in an unsteady manner. The problem is described in a rectangular coordinate system attached to the plate such that the x-axis lies along the plate surface and the y-axis is normal to the plate (Fig. 1). It is assumed that at time $\bar{t} \leq 0$, the temperatures of the plate and the micropolar fluid are maintained at the constant temperature T_∞, and at time $\bar{t} > 0$, the temperature of the plate is impulsively increased to the constant value T_w such that $T_w > T_\infty$. The continuity, momentum, micro-rotation and energy equations under the boundary layer and Boussinesq approximations can be written as:

$$\frac{\partial \bar{u}}{\partial \bar{x}} + \frac{\partial \bar{v}}{\partial \bar{y}} = 0, \tag{1}$$

$$\rho\left(\frac{\partial \bar{u}}{\partial \bar{t}} + \bar{u}\frac{\partial \bar{u}}{\partial \bar{x}} + \bar{v}\frac{\partial \bar{u}}{\partial \bar{y}}\right) = (\mu + \kappa)\frac{\partial^2 \bar{u}}{\partial \bar{y}^2} + \kappa\frac{\partial \bar{\omega}}{\partial \bar{y}} + \mathrm{g}\beta(T - T_\infty), \tag{2}$$

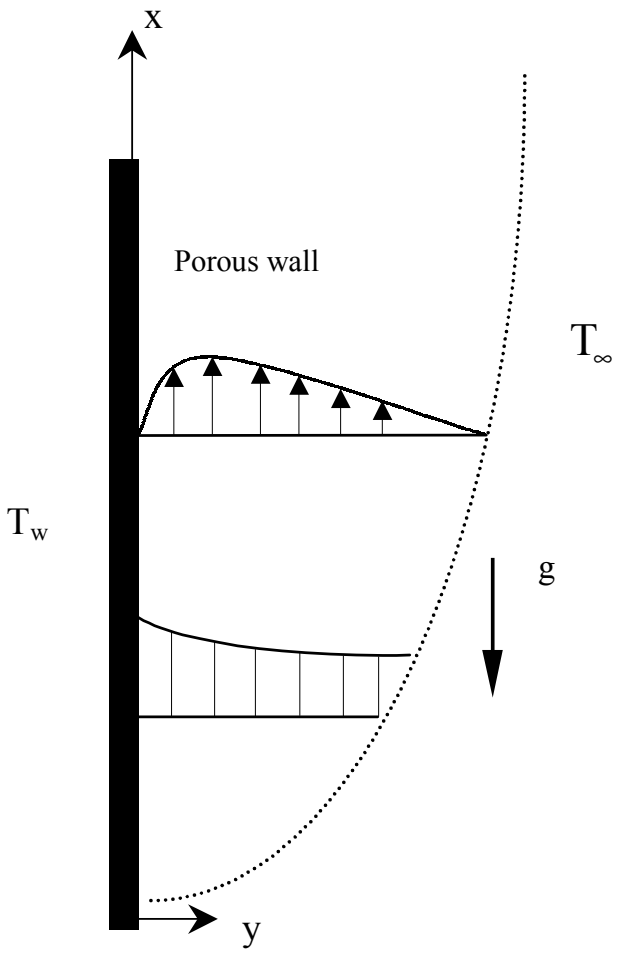

Fig. 1. The transient free convection model near a vertical wall.

$$\rho j\left(\frac{\partial\bar{\omega}}{\partial\bar{t}}+\bar{u}\frac{\partial\bar{\omega}}{\partial\bar{x}}+\bar{v}\frac{\partial\bar{\omega}}{\partial\bar{y}}\right)=-\kappa\left(\frac{\partial\bar{u}}{\partial\bar{y}}+2\bar{\omega}\right)+\gamma\frac{\partial^2\bar{\omega}}{\partial\bar{y}^2}\,, \tag{3}$$

$$\rho c_p\left(\frac{\partial T}{\partial\bar{t}}+\bar{u}\frac{\partial T}{\partial\bar{x}}+\bar{v}\frac{\partial T}{\partial\bar{y}}\right)=k\frac{\partial^2 T}{\partial\bar{y}^2}\,. \tag{4}$$

The physical initial and boundary conditions for this problem are given by:

$$\begin{aligned}
&\bar{t}\le 0: \quad \bar{u}=0,\quad \bar{v}=0,\quad \bar{\omega}=0, && T=T_\infty \quad \text{for all } \bar{x}\ge 0,\quad \bar{y}\ge 0,\\
&\bar{t}>0: \begin{cases}
\bar{u}=0,\quad \bar{v}=0,\quad \bar{\omega}=0, & T=T_\infty \quad \text{for} \quad \bar{x}=0, \quad \bar{y}\ge 0,\\
\bar{u}=0,\quad \bar{v}=0,\quad \bar{\omega}=-n(\partial\bar{u}/\partial\bar{y}), & T=T_w \quad \text{for} \quad \bar{y}=0, \quad \bar{x}\ge 0,\\
\bar{u}=0,\quad \bar{\omega}=0, & T=T_\infty \quad \text{for} \quad \bar{y}\to\infty.
\end{cases}
\end{aligned} \tag{5}$$

It should be noted that in the above boundary condition for micro-rotation variable $\bar{\omega}$ which defines its relation with the surface shear stress, the parameter n (a constant) is a number between 0 and 1 which describes the micro-rotation vector to the shear stress. The condition for which $n = 0$ corresponds to the case where the particle density is sufficiently large so that microelements close to the wall are unable to rotate. The condition for which $n = 0.5$ represents a weak representation of the microelements whereas the condition for which $n = 1.0$ corresponds to the turbulent flow inside boundary layers of micro-rotation.

Defining the non-dimensional variables such that:

$$t = \mathrm{Gr}^{1/2}(\nu/L^2)t, \qquad x = \bar{x}/L, \qquad y = \mathrm{Gr}^{1/4}(\bar{y}/L), \tag{6}$$

$$\begin{gathered} u = \mathrm{Gr}^{-1/2}(\nu/L)\bar{u}, \qquad v = \mathrm{Gr}^{-1/4}(\nu/L)\bar{v}, \\ \theta = (T - T_\infty)/(T_w - T_\infty), \qquad \omega = \bar{\omega}\mathrm{Gr}^{-3/4}(L^2/\nu) \end{gathered} \tag{7}$$

(where L is the characteristic length of the plate and $\mathrm{Gr} = \mathrm{g}\beta(T_w - T_\infty)L^3/\nu^2$ is the Grashof number) and then substituting Eq. (6) and Eq. (7) into Eqs (1) – (4) yields the following dimensionless equations:

$$\frac{\partial u}{\partial x} + \frac{\partial v}{\partial y} = 0, \tag{8}$$

$$\frac{\partial u}{\partial t} + u\frac{\partial u}{\partial x} + v\frac{\partial u}{\partial y} = (1 + R)\frac{\partial^2 u}{\partial y^2} + R\frac{\partial \omega}{\partial y} + \theta, \tag{9}$$

$$\frac{\partial \omega}{\partial t} + u\frac{\partial \omega}{\partial x} + v\frac{\partial \omega}{\partial y} = -RB\left(\frac{\partial u}{\partial y} + 2\omega\right) + \lambda\frac{\partial^2 \omega}{\partial y^2}, \tag{10}$$

$$\frac{\partial \theta}{\partial t} + u\frac{\partial \theta}{\partial x} + v\frac{\partial \theta}{\partial y} = \frac{1}{\mathrm{Pr}}\frac{\partial^2 \theta}{\partial y^2}, \tag{11}$$

where $R = \kappa/\mu$ is the vortex viscosity parameter; $B = L^2/j\mathrm{Gr}^{1/2}$ and $\lambda = \gamma/\mu j$ are dimensionless material parameters; $\mathrm{Pr} = \mu c_p/k$ is the Prandtl number.

The corresponding dimensionless initial and boundary conditions can be written as:

$$\begin{aligned} &t \le 0: && u = 0, \quad v = 0, \quad \omega = 0, && \theta = 1 && \text{for all } x \ge 0, \quad y \ge 0, \\ &t > 0: && \begin{cases} u = 0, \quad v = 0, \quad \omega = 0, & \theta = 1 & \text{for} \quad x = 0, & y \ge 0, \\ u = 0, \quad v = 0, \quad \omega = -n(\partial u/\partial y), & \theta = 1 & \text{for} \quad y = 0, & x \ge 0, \\ u = 0, \quad \omega = 0, & \theta = 0 & \text{for} \quad y \to \infty. \end{cases} \end{aligned} \tag{12}$$

The local coefficient of friction and local Nusselt number are important physical parameters for this type of flow and heat transfer situation. They can be defined in dimensionless form as:

$$C_f\mathrm{Gr}^{3/4} = (1 + R)\left.\frac{\partial u}{\partial y}\right|_{(x,0,t)} + R\omega\Big|_{(x,0,t)}, \tag{13}$$

$$\mathrm{Nu}\,\mathrm{Gr}^{-1/4} = -\left.\frac{\partial \theta}{\partial y}\right|_{(x,0,t)}. \tag{14}$$

2. Numerical Method

The transient boundary layer equations represented by Eqs (8) – (11) are solved subject to the initial and boundary conditions given by Eq. (12) using the MackCormak's method which is an explicit finite-difference technique of second-order accuracy in space and time. The details of this method of solution are clearly explained by Anderson [18]. The employed numerical solution is a time marching technique giving the downstream velocity, micro-rotation and temperature profiles using the known upstream profiles. In the present work, the above quantities have been calculated by obtaining explicitly the flow field variables at grid point (i, j) at time $t + \Delta t$ from the known flow field variables at grid points (i, j), $(i+1, j)$, $(i-1, j)$, $(i-1, j)$ and $(i, j+1)$ at time t. The flow field variables at all other grid points at time $t + \Delta t$are obtained in like fashion. Once the velocity, micro-rotation and temperature fields are obtained at a given time, then the local coefficient of friction and local Nusselt number are calculated from Eqs (13) and (14). In order to verify the accuracy of the present method, comparison of results with the similarity solutions obtained by Oosthuizen and Naylor [19] for the steady laminar free convection over a vertical isothermal impermeable plate of Newtonian fluids is performed and is shown in the Table. As is clear from it, the results are found to be in excellent agreement. This favorable comparison lends confidence in the numerical results to be reported in the next section.

3. Results and Discussion

The micropolar fluid effects on this problem are found to be proportional to material parameters and vortex viscosity parameter. The material parameter $B = L^2/j\mathrm{Gr}^{1/2}$ is found to proportional directly to the length of the plate and inversely to the micro-rotation density and the Grashof number. Also, the material parameter $\lambda = \gamma/\mu j$ is directly proportional to the spin-gradient viscosity and inversely proportional to the absolute viscosity and micro-rotation density. Note that the material parameters effects of a micropolar fluid decrease as the value of Gr or the buoyancy effect increases.

Figs 2a – c show representative dimensionless velocity profiles $u(x, y, t)$, temperature profiles $\theta(x, y, t)$ and angular or rotational velocity profiles $\omega(x, y, t)$ for different values of the vortex viscosity parameter R (0, 1, 2, 5) at fixed values of $B = 0.5$, $\mathrm{Pr} = 1.0$, $\lambda = 5$, $n = 1$, and $x = 0.5$, respectively. It should be noted that the case where $R = 0$ corresponds to Newtonian fluids. Increasing the vortex viscosity parameter has the tendency to increase the velocity and temperature inside the boundary layer and broadens the hydrodynamic and thermal boundary layer thicknesses and decreases the fluid rotation and rotational boundary layer thickness. This is due to the extra

Table 1
Values of steady state heat transfer coefficient $h(\tau = \infty, x, 0)$ along streamwise direction for air at $T_\infty = 50^\circ C$, $T_w = 10^\circ C$, $\mathrm{Pr} = 0.72$, $R = 0$, $B = 0$, $\lambda = 0$, $m = 0$.

x	Present results	Oosthuizen & Naylor [19]
0.1	10.04821	10.04088
0.2	8.44653	8.44334
0.4	7.10078	7.09997
0.6	6.45897	6.41555
0.8	6.00024	5.97034
1.0	5.700231	5.64640

mixing of fluid layers resulting from additional used shear stress.

Figs 2d and e show the variation of the local coefficient of friction $C_f\mathrm{Gr}^{3/4}$ and the local Nusselt number $\mathrm{NuGr}^{-1/4}$ against transient times for different values of the vortex viscosity parameter R (0, 1, 2, 5) and fixed values of the parameters $B = 0.5$ or 1.0, $\mathrm{Pr} = 1.0$, $\lambda = 5$, and $n = 0.5$, respectively. These figures show that the local coefficient of friction increases while the local Nusselt number decreases with dimensionless time until they reach the steady-state conditions as $\tau \to \infty$. Also, as the vortex viscosity parameter increases, the local coefficient of friction increases due higher mixing of fluid layers and increased wall slopes in the velocity and rotational velocity profiles (see Figs 2a and c) while the local Nusselt number decreases due to excessive heating of fluid layers. It is also observed from these figures that while the changes in the local coefficient of friction due to changes in the values of R occur at any given dimensionless time, the same is not true for the local Nusselt number in which the variations are limited to large value of time (steady-state range). These behaviors are clearly shown in Figs 2d and e.

Fig. 2f displays the changes of the local coefficient of friction $C_f\mathrm{Gr}^{3/4}$ along the streamwise direction or distance along the plate x for different values of R. It is clearly observed that the local coefficient of friction increases as the streamwise distance increases. Also, as explained above the values of $C_f\mathrm{Gr}^{3/4}$ increase as R increases due to increased wall velocity and rotational velocity gradients.

Figs 3a – c present typical dimensionless velocity profiles $u(x, y, t)$, temperature profiles $\theta(x, y, t)$ and angular velocity profiles $\omega(x, y, t)$ for different values of the dimensionless material parameter B (0.1, 0.3, 0.6, 1.0) and fixed values of other parameters $R = 1.0$, $\mathrm{Pr} = 1.0$, $\lambda = 5$, $n = 1$, and $x = 0.5$, respectively. The increasing of dimensionless material parameter B decreases the fluid velocity inside the boundary layer. This is due to the retarding effect of the micro-inertia density resulting in smaller buoyancy forces. This is similar to a flow against an adverse pressure gradient situation. Also, as the dimensionless material parameter B increases, the fluid rotation inside the boundary layer increases because of favorable non-Newtonian effects while this increase has negligible effects on the temperature profiles.

Figs 3d and e illustrate the effects of varying the dimensionless material parameter B on the time development of both the local coefficient of friction and local Nusselt number, respectively. Increasing the value of B increases the coefficient of friction due to increased wall gradients in the velocity and rotational velocity profiles while it has negligible effects on Nusselt number due to insignificant changes in the temperature profiles. These figures also show the proper transition of $C_f\mathrm{Gr}^{3/4}$ and $\mathrm{NuGr}^{-1/4}$ to steady-state conditions.

Fig. 3f shows the development of the local coefficient of friction $C_f\mathrm{Gr}^{3/4}$ along the distance along the plate x for different values of B. Again, the local coefficient of friction increases as the streamwise distance increases. Also, as mentioned above the values of $C_f\mathrm{Gr}^{3/4}$ increase as B increases due to increased wall slopes of the velocity and rotational velocity profiles.

Figs 4a – c show the effect of the dimensionless micro-gyration parameter m on the angular velocity profiles and the time development of local coefficient of friction and local Nusselt number, respectively. As the dimensionless micro-gyration parameter increases, the fluid rotation (or angular velocity) inside the boundary layer as well as the local coefficient of friction at any specific time decrease while the local values of Nusselt number at any specific time enhance. This is due to excessive angular momentum within fluid layers.

Fig. 4d displays the development of the local coefficient of friction $C_f\mathrm{Gr}^{3/4}$ along the streamwise direction x for different values of m. It is clearly observed that the local coefficient of friction increases as the streamwise distance increases while it decreases as n increases due to decreased

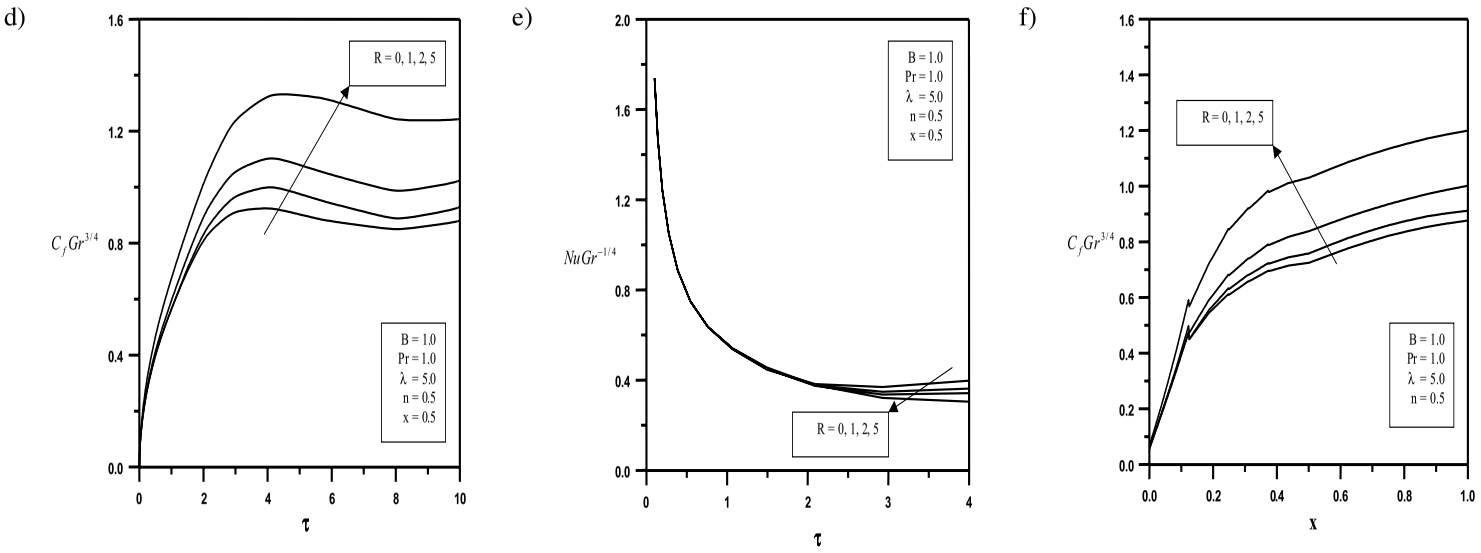

Fig. 2. Physical quantities for different values of the vortex viscosity parameter R:
a) dimensionless steady state velocity profiles; b) dimensionless steady state temperature profiles;
c) dimensionless steady state angular velocity profiles; d) time development of local coefficient of friction;
e) time development of local Nusselt number; f) streamwise development of steady state local coefficient of friction.

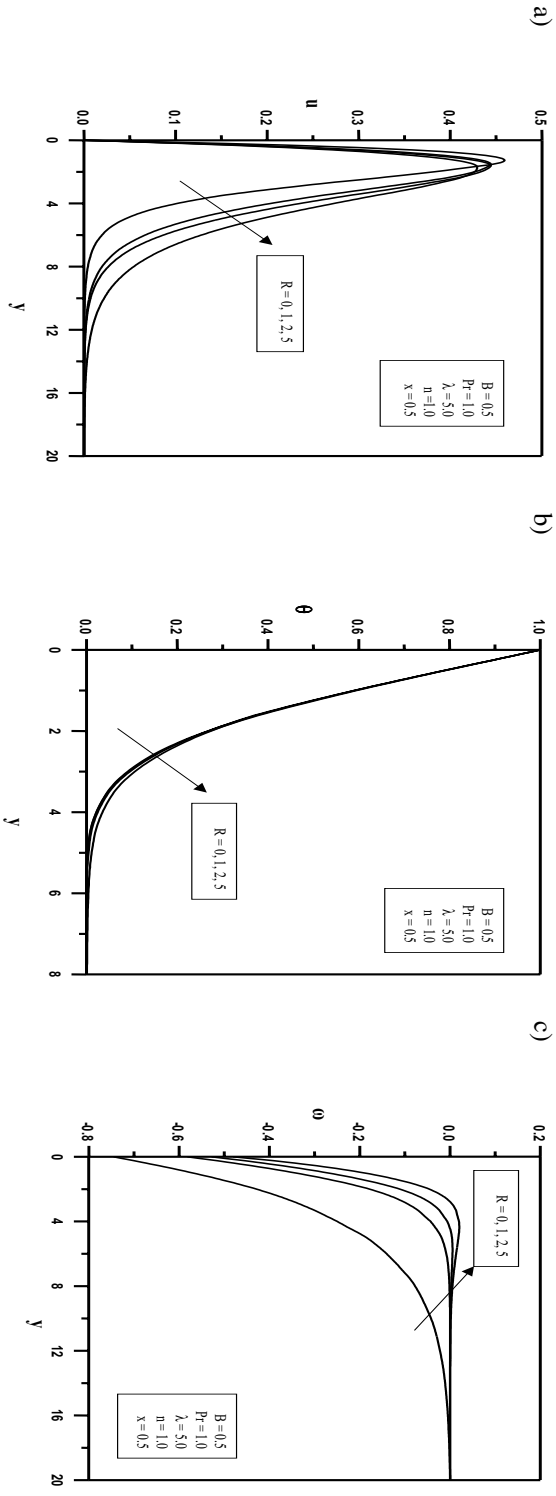
a)
u
y
R = 0, 1, 2, 5
B = 0.5
Pr = 1.0
λ = 5.0
n = 1.0
x = 0.5
b)
θ
y
R = 0, 1, 2, 5
B = 0.5
Pr = 1.0
λ = 5.0
n = 1.0
x = 0.5
c)
ω
y
R = 0, 1, 2, 5
B = 0.5
Pr = 1.0
λ = 5.0
n = 1.0
x = 0.5

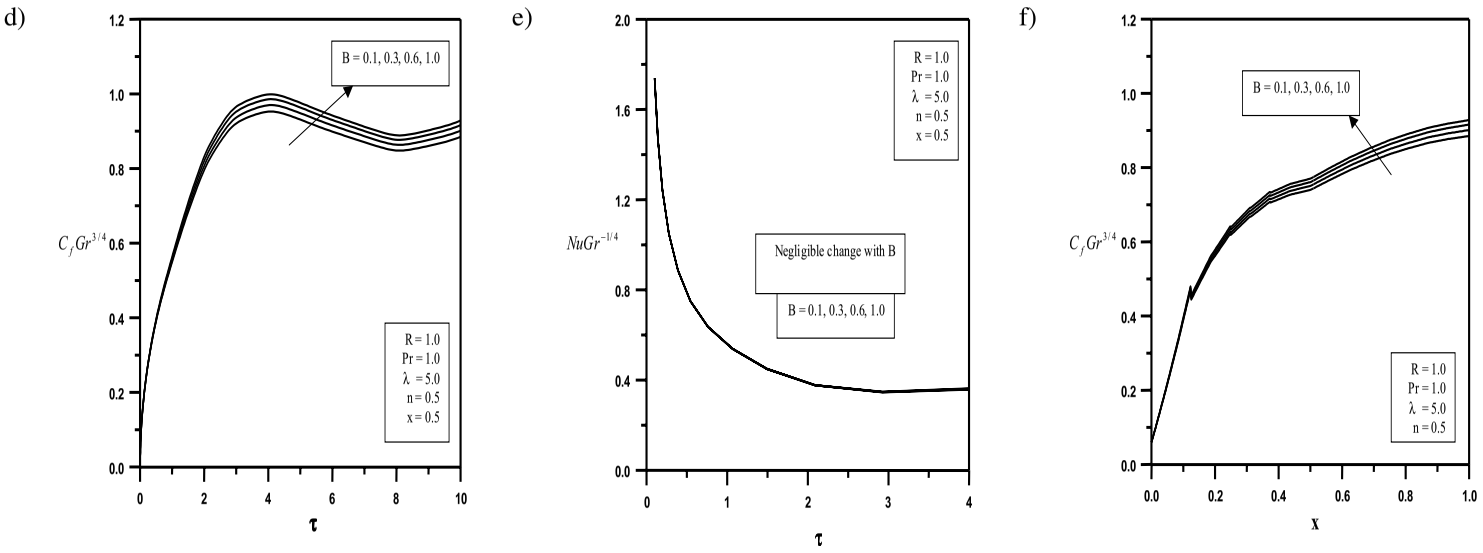

Fig. 3. Physical quantities for different values of the material parameter B:
a) Dimensionless steady state velocity profiles; b) dimensionless steady state temperature profiles;
c) dimensionless steady state angular velocity profiles; d) time development of local coefficient of friction;
e) time development of local Nusselt number; f) streamwise development of steady state local coefficient of friction.

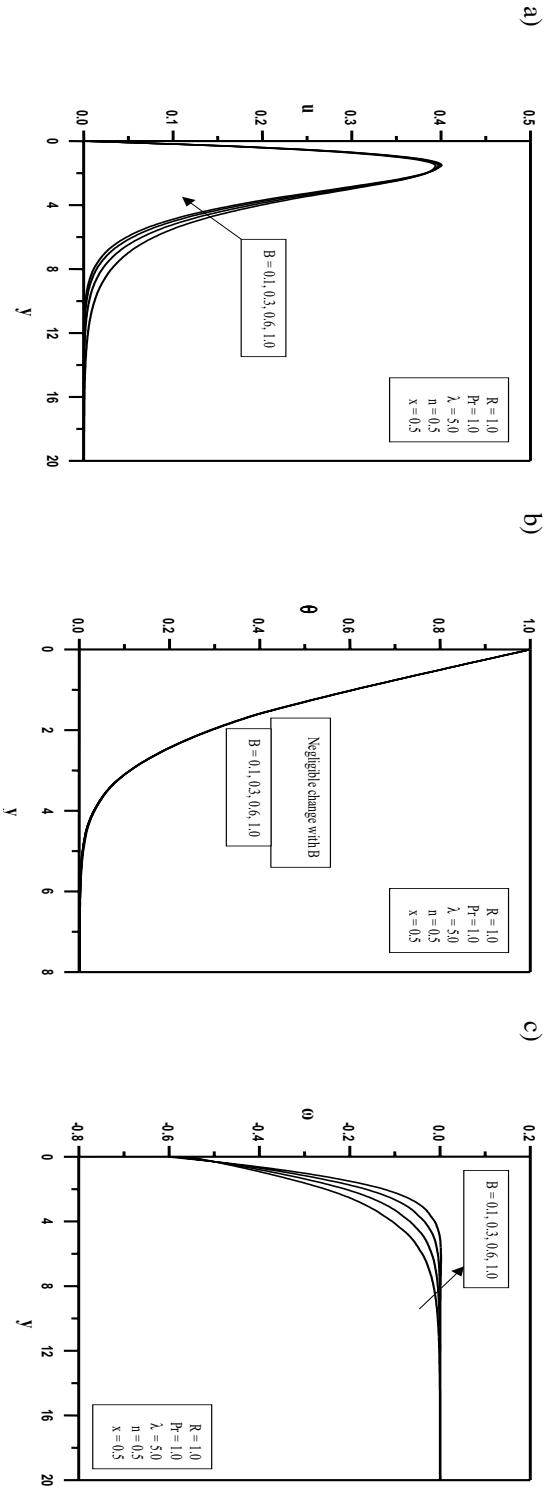
a)
u
y
B = 0.1, 0.3, 0.6, 1.0
R = 1.0
Pr = 1.0
λ = 5.0
n = 0.5
x = 0.5
b)
θ
y
Negligible change with B
B = 0.1, 0.3, 0.6, 1.0
R = 1.0
Pr = 1.0
λ = 5.0
n = 0.5
x = 0.5
c)
ω
y
B = 0.1, 0.3, 0.6, 1.0
R = 1.0
Pr = 1.0
λ = 5.0
n = 0.5
x = 0.5

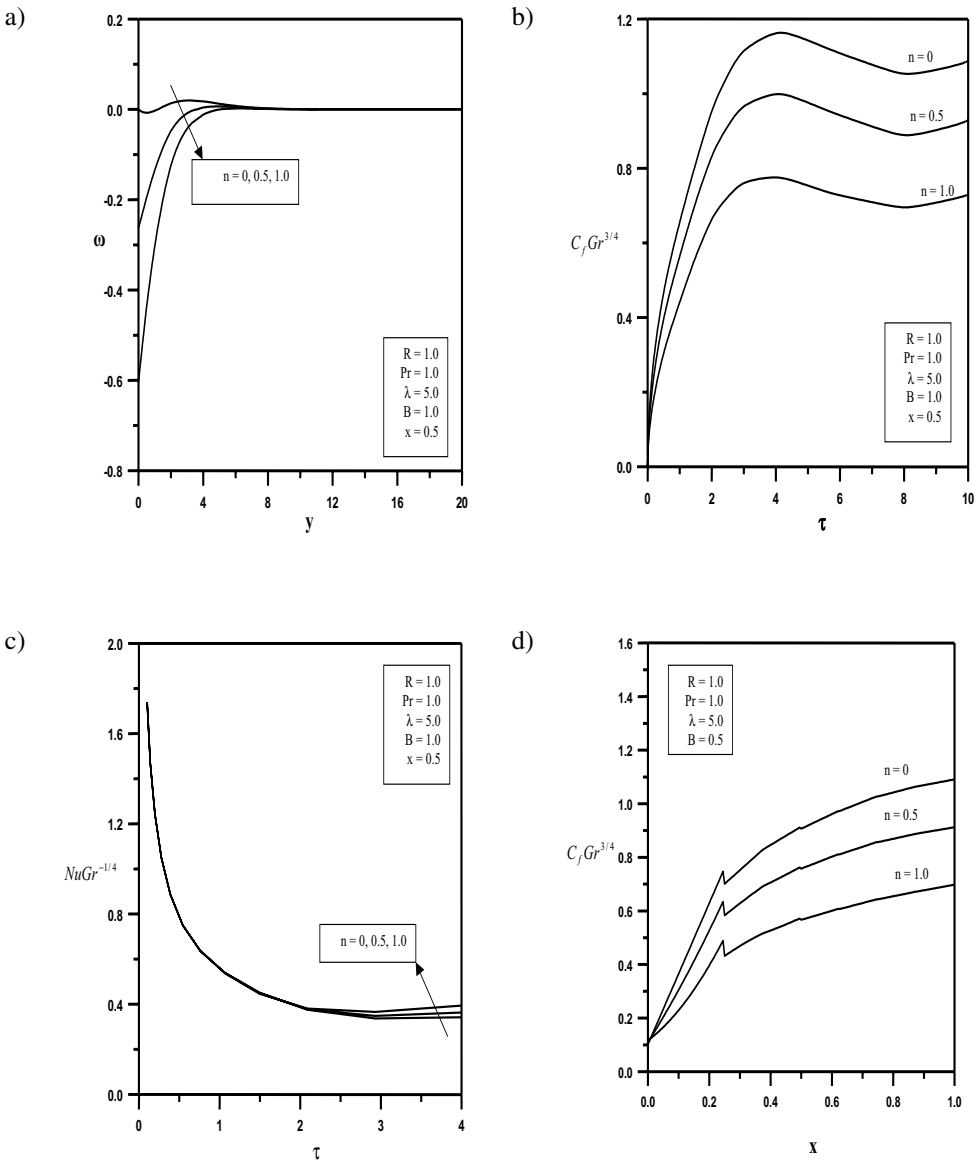

Fig. 4. Physical quantities for different values of the micro-gyration parameter n:
a) dimensionless steady state angular velocity profiles;
b) time development of local coefficient of friction;
c) time development of local Nusselt number;
d) streamwise development of steady state local coefficient of friction.

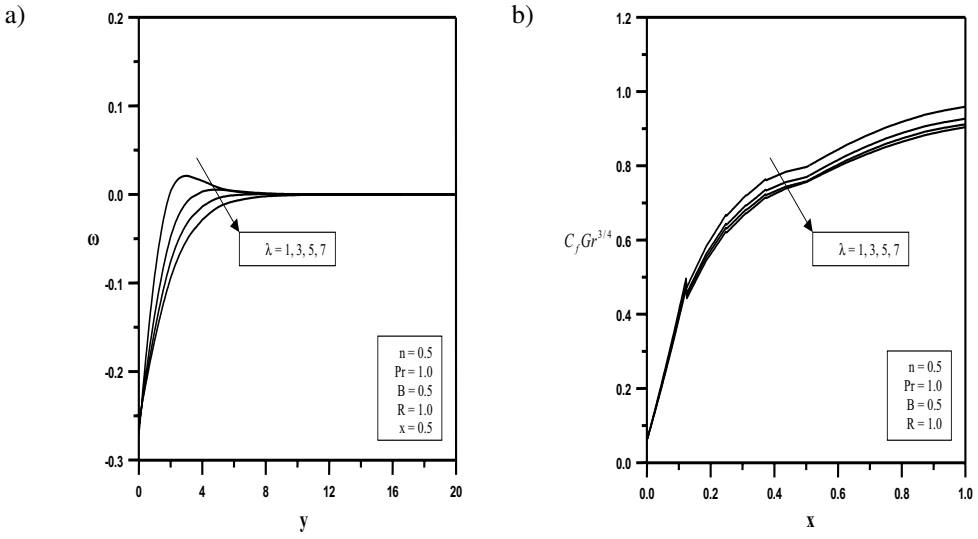

Fig. 5. Physical quantities for different values of the material parameter λ:
a) dimensionless steady state angular velocity profiles;
b) streamwise development of steady state local coefficient of friction.

wall velocity and rotational velocity gradients.

Finally, the effects of the dimensionless material parameter λ which represents the spin-gradient viscosity on both the angular velocity profiles and the local coefficient of friction are presented in Figs 5a and b, respectively. It is clear from these figures that increasing the material parameter λ decreases the fluid rotation inside the boundary layer as well as the local coefficient of friction.

Conclusions

The transient laminar free convection heat transfer effects from a vertical surface for a micropolar fluid were studied. The governing equations were written in dimensionless form using a set of variables and then solved using an explicit finite-difference technique. Comparisons with previously published work were performed and found to be in excellent agreement. It was found that as the micro-gyration parameter increased, the local coefficient of friction at any specific time decreased while the local Nusselt number increased. On the other hand, as the vortex viscosity parameter was increased, the local coefficient of friction was enhanced while the local Nusselt number was decreased especially close to the steady state conditions. Also, increasing the micropolar material parameter was found to increase the coefficient of friction while it had a negligible effect on the local Nusselt number.

REFERENCES

1. Eringen, A. C., Theory of Micropolar Fluids, *J. Math. Mech.*, 1966, **16**, pp. 1–18.
2. Eringen, A. C., Theory of Thermomicropolar Fluids, *J. Math. Anal. Appl.*, 1972, **38**, pp. 480–496.

3. Ariman, T., Turk, M. A., and Sylvester, N. D., Microcontinuum Fluid Mechanics – A Review, *Int. J. Engng Sci.*, 1973, **11**, pp. 905–930.
4. Ariman, T., Turk, M. A., and Sylvester, N. D., Applications of Microcontinuum Fluid Mechanics – A Review, *Int. J. Engng Sci.*, 1974, **12**, pp. 273–293.
5. Ahmadi, G., Self-Similar Solution of Incompressible Micro-Polar Boundary Layer Flow over a Semi-Infinite Plate, *Int. J. Engng Sci.*, 1976, **14**, pp. 639–646.
6. Gorla, R. S. R., Pender, R., and Eppich, J., Heat Transfer in Micropolar Boundary Layer Flow Over a Flat Plate, *Int. J. Engng Sci.*, 1983, **21**, pp. 791–798.
7. Agarwal, R. S. and Dhanapal, C., Flow and Heat Transfer in a Micropolar Fluid Past a Flat Plate with Suction and Heat Sources, *Int. J. Engng Sci.*, 1988, **26**, pp. 1257–1266.
8. Lien, F. S., Chen, C. K., and Cleaver, J. W., Analysis of Natural Convection Flow of Micropolar Fluid About a Sphere with Blowing and Suction, *ASME J. Heat Tranfer*, 1986, **108**, pp. 967–970.
9. Lien, F. S., Chen, T. M., and Chen, C. K., Analysis of Free-Convection Micropolar Boundary Layer About a Horizontal Permeable Cylinder at a Non-Uniform Thermal Condition, *ASME J. Heat Transfer*, 1990, **112**, pp. 504–506.
10. Yao, L. S., Natural Convection along a Vertical Wavy Surface, *ASME J. Heat Transfer*, 1983, **105**, pp. 464–468.
11. Cheng, C. Y. and Wang, C. C., Forced Convection in Micropolar Fluid Flow Over a Wavy Surface, *Numer. Heat Transfer, A*, 2000, **37**, pp. 271–287.
12. Bhargava Rama and Takhar, H. S., Numerical Study of Heat Transfer Characteristics of the Micropolar Boundary Layer Near a Stagnation Point on a Moving Wall, *Int. J. Engng Sci.*, 2000, **38**, pp. 383–394.
13. Mansour, M. A., Alhakiem, M. A., and El Kabeir, S. M., Heat and Mass Transfer in Magnetohydrodynamic Flow of Micropolar Fluid on a Circular Cylinder with Uniform Heat and Mass Flux, *J. Magnetism Magnet. Mater.*, 2000, **220**, pp. 259–270.
14. Kelson, N. A. and Desseaux, A., Effect on Surface Conditions on Flow of a Micropolar Fluid Driving by a Porous Stretching Sheet, *Int. J. Engng Sci.*, 2001, **39**, pp. 1881–1897.
15. Ibrahim, F. S. and Hassanien, I. A., Local Nonsimilarity Solutions for Mixed Convection Boundary Layer Flow of a Micropolar Fluid on Horizontal Flat Plates with Variable Surface Temperatures, *Appl. Math. Comput.*, 2001, **122**, pp. 133–153.
16. Kim, Y. J. and Lee, J. C., Analytical Studies on MHD Oscillatory Flow of a Micropolar Fluid Over a Vertical Porous Plate, *Surf. Coat. Technol.*, 2003, **171**, pp. 187–193.
17. Elbarbary, E. M. E. and Elgazery, N. S., Chebyshev Finite Difference Method for the Effects of Variable Viscosity and Variable Thermal Conductivity on Heat Transfer from Moving Surfaces with Radiation, *Int. J. Thermal Sci.*, 2004, **43**, pp. 889–899.
18. Anderson, J. D., *Computational Fluid Dynamics*, McGraw-Hill, New York, 1995.
19. Oosthuizen, P. H. and Naylor, D., *An Introduction to Convective Heat Transfer*, McGraw-Hill, New York, 1999.

□◆◆◆□